ORIGINAL ARTICLE

In Vivo Quantification of Cerebral R2*-Response to Graded Hyperoxia at 3 Tesla

Grigorios Gotzamanis[1,2], Roman Kocian[3], Pinar S. Özbay[1,4], Manuel Redle[1], Spyridon Kollias[5], Christian Eberhardt[1], Andreas Boss[1], Daniel Nanz[1], Cristina Rossi[1]

[1]Departments of Diagnostic and Interventional Radiology, [3]Anesthesiology, and [5]Neuroradiology, University Hospital of Zurich, [4]Institute for Biomedical Engineering, Eidgenössische Technische Hochschule (ETH), Zurich, Switzerland, [2]Klinikum Dritter Orden, Center for Radiology and Nuclear Medicine, Munich, Germany

Address for correspondence:
Dr. Cristina Rossi,
Department of Diagnostic and
Interventional Radiology, University
Hospital Zurich, Raemistrasse 100,
Zurich - CH-8091, Switzerland.
E-mail: cristina.rossi@usz.ch

ABSTRACT

Objectives: This study aims to quantify the response of the transverse relaxation rate of the magnetic resonance (MR) signal of the cerebral tissue in healthy volunteers to the administration of air with step-wise increasing percentage of oxygen. **Materials and Methods:** The transverse relaxation rate (R2*) of the MR signal was quantified in seven volunteers under respiratory intake of normobaric gas mixtures containing 21, 50, 75, and 100% oxygen, respectively. End-tidal breath composition, arterial blood saturation (SaO_2), and heart pulse rate were monitored during the challenge. R2* maps were computed from multi-echo, gradient-echo magnetic resonance imaging (MRI) data, acquired at 3.0T. The average values in the segmented white matter (WM) and gray matter (GM) were tested by the analysis of variance (ANOVA), with Bonferroni *post-hoc* correction. The GM R2*-reactivity to hyperoxia was modeled using the Hill's equation. **Results:** Graded hyperoxia resulted in a progressive and significant ($P < 0.05$) decrease of the R2* in GM. Under normoxia the GM-R2* was 17.2 ± 1.1 s^{-1}. At 75% O_2 supply, the R2* had reached a saturation level, with 16.4 ± 0.7 s^{-1} ($P = 0.02$), without a significant further decrease for 100% O_2. The R2*-response of GM correlated positively with CO_2 partial pressure ($R = 0.69 \pm 0.19$) and negatively with SaO_2 ($R = -0.74 \pm 0.17$). The WM showed a similar progressive, but non-significant, decrease in the relaxation rates, with an increase in oxygen intake ($P = 0.055$). The Hill's model predicted a maximum R2* response of the GM, of 3.5%, with half the maximum at 68% oxygen concentration. **Conclusions:** The GM-R2* responds to hyperoxia in a concentration-dependent manner, suggesting that monitoring and modeling of the R2*-response may provide new oxygenation biomarkers for tumor therapy or assessment of cerebrovascular reactivity in patients.

Key words: Blood oxygen level dependent (BOLD), graded hyperoxia, R2*, respiratory challenge

Access this article online	
Quick Response Code:	
	Website: www.clinicalimagingscience.org
	DOI: 10.4103/2156-7514.150439

INTRODUCTION

Increasing the oxygen supply by administration of hyperoxic gas mixtures induces detectable changes in the magnetic

resonance (MR) signal measured in the T2*-weighted images.[1,2] This blood oxygen level dependent (BOLD) effect mainly and indirectly reflects the manipulated deoxyhemoglobin concentration in the capillary bed of the tissue.[3,4]

Respiratory challenges are used in calibrated functional MRI experiments to quantify the cerebral metabolic rate of oxygen.[5-7] The noninvasive monitoring of the response of tissue to hyperoxia may also find a clinical application in the assessment of cerebrovascular reactivity (CVR) in patients, and in the investigation of the potential benefits of oxygen treatment in acute care and in ischemia.[8-10] In general, CVR is the ability of the cerebral vasculature to respond to an external stimulus, which may affect both the cerebral blood flow (CBF) and the cerebral blood volume (CBV).[11] Non-invasively, CVR is most commonly measured by Arterial Spin Labeling, which quantifies tissue perfusion using magnetically labeled arterial blood, however, typically with a rather low signal-to-noise ratio. BOLD imaging is also increasingly used to measure CVR.[12] In a BOLD measurement, the signal intensity decreases with the increasing content of deoxyhemoglobin within the measured voxel. This signal drop is caused by faster signal dephasing on account of the paramagnetic properties of deoxyhemoglobin and concomitant microscopic magnetic field inhomogeneities. With increasing blood flow, deoxyhemoglobin is more diluted, which results in an increased BOLD signal; therefore, the BOLD signal is an indirect measure of CVR. The BOLD signal is related to quantitative R2* changes depending on the applied BOLD sequence type and parameters. For respiratory challenges, the mutual influence of oxygen saturation/oxygen affinity and CO_2 concentration/pH in the blood stream (Haldane effect) needs to be taken into account.[13,14] The CVR can be measured using both, oxygen and CO_2 challenges, or carbogen, which is a mixture of oxygen and CO_2.[11,12]

The main field of clinical application is related to monitoring the oxygenation status of tumor cells in radiotherapy-resistant tumors during administration of hyperoxic gas mixtures.[15-17] The proposed therapeutical approach relies on an increase in the amount of dissolved oxygen in the plasma to induce oxygen diffusion into the pathological hypoxic regions.[16]

In spite of the growing popularity of this approach in neuroscience, the possibility of manipulating tissue oxygenation by increasing the oxygen supply is still a matter of debate as several compensating mechanisms (e.g. increase in blood pressure, increase in vascular resistance, heart rate decrease) occur when increasing the fraction of inspired oxygen.[10]

A significant negative correlation between the BOLD signal and the deoxyhemoglobin concentration was reported in a preclinical study on neonatal piglets, and it was suggested that tissue oxygenation could indeed be manipulated by increasing the oxygen supply.[18] As the concentration of the oxygenated hemoglobin varied with the partial pressure of oxygen (ppO_2) in the tissue, T2* (or equivalently R2* =1/T2*) could be considered as an indirect marker of tissue oxygenation.[16]

Two key factors affect the R2* response to hyperoxic respiratory challenges: the strength of the static magnetic field and the amount of oxygen delivered. In a recent study, a quadratic dependence of the respiratory-challenge induced R2* change in the cerebral gray matter on the strength of the static magnetic field was reported for intake of pure oxygen and carbogen.[2] The study suggested that highly resolved mapping of the R2* may mainly reflect the response of the microvasculature (i.e. of vessels with a radius smaller than 8 μm) to the challenge.

In our study, we have focused on the dependence of the R2* response to the concentration of delivered oxygen. The aim of this study was to quantify and model the BOLD response in terms of changes in the relaxation rate R2* of the MR signal of the cerebral tissue under graded hyperoxia, in healthy volunteers.

MATERIALS AND METHODS

Subjects
Seven young healthy volunteers (mean age 24.0 ± 1.3 years, four males and three females) without any history of respiratory, cardiovascular, or neurological disease were enrolled in the study. The subjects gave a written informed consent for the MR examination and the scientific evaluation of the datasets. The study was approved by the Institutional Review Board (IRB). All procedures were performed in accordance with the Helsinki Declaration.

Breathing system and gas administration protocol
Variable amounts of medical air and pure oxygen were mixed to achieve normobaric gas compositions containing oxygen percentages of 21, 50, 75, and 100%, respectively. Gas mixture and delivery, as well as measurements of the partial pressures of CO_2 ($ppCO_2$) and O_2 (ppO_2) in the end-tidal gas were performed using an MR-compatible anesthesia machine (Fabius MRI, Draeger Medical GmbH, Germany). During the whole examination an experienced anesthesiologist remained in the MR room and adjusted the setting on the anesthetic device accordingly. The gases were administered according to the following paradigm: Six minutes medical air (i.e. 21% oxygen), six minutes 50% oxygen, six minutes 75% oxygen, and six minutes 100% oxygen. To account for the time lag of the response to

the hyperoxic challenge, image acquisition was started three minutes after the initiation of gas inhalation for each step.[19,20]

During the whole MR-examination volunteers were requested to wear an injectable air cushion facial mask with a hook valve (Dahlhausen, Cologne, Germany) connected to the anesthesia machine, and to breathe normally. The gas flow was set to 10–15 liters per minute. During the measurements, arterial blood saturation and heart pulse rate were monitored using an MR-compatible fingertip pulse oximeter. Tidal CO_2 and O_2 partial pressures were monitored during the challenges. For end-tidal partial pressures, arterial blood saturation and pulse rate and the minimum and maximum values registered during each stage of the challenge have been registered.

Magnetic Resonance protocol

Magnetic Resonance data were acquired using a 3.0 Tesla scanner (Philips Ingenia, Philips Medical Systems, Best, Netherland). The signal was received via an eight-channel head coil. The built-in body transmit coil was used for spin excitation. To minimize motion, foam paddings were positioned between the coil former and the subjects' heads.

Two-dimensional T1-weighted spin-echo images were acquired (Time to Repetition, TR = 600 ms, Time to Echo, TE = 10 ms, Flip Angle, FA = 70°, voxel size = 0.6 × 0.6 × 4.0 mm^3) during medical air breathing, in transverse and sagittal orientations, as anatomical references. During each stage of the respiratory challenge, a three-dimensionally encoded, multi-echo, radiofrequency-spoiled gradient echo (GRE) sequence was scanned (FA = 50°, TR = 93 ms, TE = 8, 24, 40, 56, 72, 88 ms, voxel size = 0.5 × 0.5 × 1.0 mm^3). Ten transversal slices were positioned tangentially to and above the corpus callosum.

Magnetic Resonance data processing

Magnetic Resonance images were processed offline using the in-house custom software that was written in the programming languages Python (Python Software Foundation, version 2.7.) and Matlab (MATLAB Release 2009b, the MathWorks, Inc., Natick, Massachusetts, United States).

R_2* quantification

For each stage of the challenge, the BOLD response was quantified by pixel-wise computation of the transverse rate of relaxation of the MR signal, R2*. The data were linearized by taking the logarithm of the MR-signal intensities. To minimize the potential bias and the disproportionate weight of low-intensity data, the data-point weights that exponentially decayed with TE, given by the mean signal at the given TE averaged over all image pixels, were used. The MR signal was fitted to the expression:

$$\ln(S(TE)) = \ln(S_0) - R_2^* \cdot TE \qquad (1)$$

using the 'polyfit' algorithm of the numpy package, version 1.7.1 (Scipy.org) with S representing the signal intensity of the magnitude image, S_0 the signal intensity at zero echo time, and TE the time to echo.[21] The fitting variables were S_0 and R2*.

Tissue segmentation

Three-dimensional MR images of the brain were segmented into GM, WM, and cerebral spinal fluid (CSF) using the FMRIB (Functional MRI of the Brain) Software Library.[22,23] The FMRIB Automated Segmentation Tool (FAST) relies on a Markov random field (MRF) model and on an algorithm for maximization of the associated expectation.[22]

Statistical analysis

Intra-subject analysis

The mean R2* values (and standard deviations) were computed over the whole cohort of subjects for the GM and the WM at each step of the challenge. The mean R2* values were computed over the segmented R2* maps.

In order to normalize the R2* values to the individual oxygen saturation levels, the ratio R2*/SaO_2 was computed for each subject and for each stage of the challenge (average of minimum and maximum SaO_2 of the plateau steady state).

Inter-subject analysis

To account for inter-subject variation of the baseline normoxia relaxation rates, the relative change was computed for each step of the challenge as follows:

$$\Delta R_2^* = (R_{2,challenge}^* - R_{2,normoxia}^*) / R_{2,normoxia}^* \qquad (2)$$

The monitored physiological parameters and the computed relaxation rates were statistically tested for correlation by means of 1-way ANOVA analysis with post-hoc Bonferroni correction for multiple comparisons between different challenges. The R2* values of each breathing gas composition was compared to all other gas compositions applying a significance level of 0.05.

The Bonferroni-corrected ΔR2* response to the challenge of the GM as a function of the relative increase in oxygen supply as compared to normoxia ($Stimulus = \frac{O_2[\%] - 21}{21}$) was modeled using a two-parameter saturation growth curve known as the Hill's equation:[24]

$$-\Delta R_{2,Bonferroni}^* = \frac{A \cdot Stimulus}{B + Stimulus} . \qquad (3)$$

In the delineated formula the intensity of the response is a fixed proportion of the maximum response *A* to the stimulus and *B* is the stimulus that induces a response equal to half of the maximum. Therefore, A corresponds to the maximum Δ R2* response at saturation and B describes the oxygen concentration in the breathing gas, resulting in 50% of the maximum response. The curve parameters were estimated using the *nlinfit* function of Matlab.

RESULTS

Physiological parameters

The mean values of the physiological parameters monitored during the challenge and the results of the analysis of the R2* maps, are summarized in Tables 1 and 2, respectively. The graded increase in oxygen supply resulted in a slight, but significant ($P < 0.005$) increase in the arterial hemoglobin saturation from $97.5 \pm 1.0\%$ (under normoxia) to $99.6 \pm 0.5\%$ (while breathing 100% O_2). The increasing oxygen concentration of the inhaled breathing gas also caused a statistically significant decrease in the end-tidal ppCO$_2$, from 5.8 ± 0.2 kPa under normoxia to 5.1 ± 0.4 kPa measured during breathing of 100% oxygen ($P < 0.005$). The mean pulse rate decreased during the MR examination from 68 ± 13 under normoxia to 62 ± 9 beats per minute measured during breathing of 100% oxygen.

Magnetic Resonance image quality

R2* maps were computed over the whole cohort of subjects and during each stage of the challenge. In one of the healthy volunteers, the image artifacts arising across the whole slab compromised the R2* quantification results. For this reason, this volunteer was not included in the data analysis. Image artifacts, potentially arising from the imperfection of the slab profile of the radiofrequency excitation pulse, were also observed at the border of the 3D imaging volume for other volunteers.[25] However, as the central slices presented a good image quality, which allowed for both, R2* quantification and tissue segmentation, at all steps of the challenge [Figure 1], the data reported in Table 2 was computed over tissue segmented in the five central slices of the 3D slab.

R2* response to the respiratory challenge

Under normoxia, the mean R2* values of 17.2 ± 1.1 s^{-1} and of 18.9 ± 0.6 s^{-1} were measured in GM and WM, respectively.

In Table 3, the results of the ANOVA analysis using multi-comparison tests are provided. The intra-individual analysis showed that in GM the increase in the oxygen supply resulted in a decrease of the R2* values [Figures 2 and 3], whereas, a maximum decrease in the R2* of the GM, as compared to normoxia, was observed during breathing of 75% oxygen (R2* $=16.4 \pm 0.7$ s^{-1}). Increasing the oxygen supply from 21 to 50% resulted in a mean relative R2* change of -2.3 $\pm$2.2%. The further increase in oxygen supply to 75% caused a higher R2* relative change of -4.7 $\pm$4.1%, as compared to normoxia. Breathing of 100% produced a comparable effect on the relaxation rate of the GM, as in the previous stage of the challenge (ΔR2* = -3.9 $\pm$ 2.8 %.).

Table 1: Physiological parameters monitored during the challenge

Subject	21% O$_2$			50% O$_2$			75% O$_2$			100% O$_2$		
	ppCO$_2$* [kPa]	SaO$_2$* [%]	Pulse rate [bpm]	ppCO$_2$ [kPa]	SaO$_2$ [%]	Pulse rate [bpm]	ppCO$_2$ [kPa]	SaO$_2$ [%]	Pulse rate [bpm]	ppCO$_2$ [kPa]	SaO$_2$ [%]	Pulse rate [bpm]
1	5.60	97.5	65	5.40	99.5	59	4.90	99.0	60	4.80	99.5	61
2	6.10	96.5	74	5.80	99.0	64	5.65	99.0	63	5.45	99.0	63
3	5.85	96.5	62	5.35	99.5	62	4.70	100.0	60	4.85	100.0	66
4	5.70	98.5	82	5.50	99.5	73	5.15	100.0	72	5.20	100.0	71
5	5.75	99.0	77	5.35	100	65	4.95	100.0	63	4.80	100.0	66
6	5.95	97.0	47	5.8	99.0	44	5.80	100.0	45	5.60	99	46
Mean ± SD	5.8 ± 0.2	97.5 ± 1.0	68 ± 13	5.5 ± 0.2	99.4 ± 0.4	61 ± 10	5.2 ± 0.4	99.7 ± 0.5	60 ± 9	5.1 ± 0.4	99.6 ± 0.5	62 ± 9

*The mid-range (i.e., (Max. Value+min. Value)/2) is listed in the table. SD: Standard deviation

Table 2: Normoxic mean R2* values and relative R2* deviations from the normoxic value (ΔR2*, (equation [2])) computed for white and gray matter

	Gray matter				White matter			
	21% O$_2$	50% O$_2$	75% O$_2$	100% O$_2$	21% O$_2$	50% O$_2$	75% O$_2$	100%
Subject	R2*	ΔR2*	ΔR2*	ΔR2*	R2*	ΔR2*	ΔR2*	ΔR2*
1	18.1 ± 0.4	− 2.2	− 3.3	− 2.2	17.9 ± 1.6	3.0	− 2.7	0.3
2	17.3 ± 0.1	0.3	− 1.9	− 2.3	19.1 ± 0.4	− 1.3	− 2.1	− 3.6
3	18.6 ± 0.9	− 0.1	− 10.6	− 8.5	19.2 ± 0.4	− 0.1	− 0.8	− 0.5
4	16.6 ± 0.1	− 2.8	− 2.8	− 1.7	18.4 ± 0.8	− 0.7	− 0.2	− 2.3
5	15.7 ± 0.2	− 3.3	− 0.6	− 2.4	18.9 ± 0.2	− 3.0	− 3.9	− 4.9
6	17.3 ± 1.0	− 5.7	− 9.0	− 6.2	19.7 ± 1.8	− 5.6	− 10.8	− 13.9
Mean ± SD	17.2 ± 1.1	− 2.3 ± 2.2	− 4.7 ± 4.1	− 3.9 ± 2.8	18.9 ± 0.6	− 1.3 ± 2.9	− 3.4 ± 3.9	− 4.1 ± 5.1

SD: Standard deviation

The inter-subject and the intra-subject analysis of the R2* values over the white matter showed a trend toward lower values from normoxia to the administration of 100% O_2 ($R2*_{normoxia}$ = 18.9 ± 0.6 s^{-1}, $R2*_{100\%}$ =18.1 ± 0.7 s^{-1}). However, the relaxation-rate decrease was not statistically significant.

R2* measurements versus physiological parameters

The R2*-response of the GM showed a positive correlation with the $ppCO_2$ (mean correlation coefficient 0.69 ± 0.19) and a negative correlation with the SaO_2 (mean correlation coefficient -0.74 ± 0.17). The dependence of the ratio between the R2* and the SaO_2 on the fraction of inhaled oxygen (FiO_2) is reported in Figure 4. By increasing the oxygen supply from 21 to 50% a decrease of the $R2*/SaO_2$

Table 3: ANOVA analysis of the R2* values

Bonferroni's multiple comparison test	Mean difference [s^{-1}]	t value	95% confidence interval
21 vs. 50%	1.490*	4.048	0.373-2.607
21 vs. 75%	1.630*	4.429	0.513-2.747
21 vs. 100%	2.357*	6.403	1.239-3.474
50 vs. 75%	0.140	0.380	-0.978-1.257
50 vs. 100%	0.867	2.355	-0.251-1.984
75 vs. 100%	0.727	1.974	-0.391-1.844

*Statistical significance ($p < 0.05$)
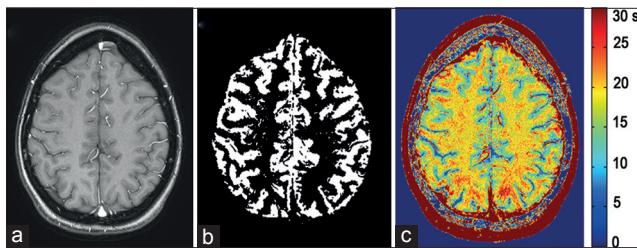
Figure 1: Axial brain images acquired above the body of the lateral ventricle from a typical volunteer are displayed. (a) T1-weighted anatomical reference image acquired using an MR gradient echo sequence (TR/TE =93ms/8ms, Flip Angle =50°, voxel size =0.5 × 0.5 × 1.0 mm^3), (b) the corresponding gray matter segmentation mask, and (c) the parametrical R2* map (computed from the pixel-wise fitting of multi-echo MR signals acquired using a gradient echo sequence) of one of the healthy volunteers under normoxia (i.e. during inhalation of medical air with 21% O_2).
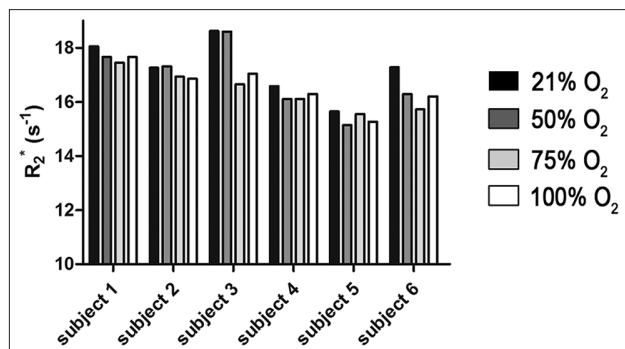
Figure 3: Visual representation of the gray-matter R2* relaxation rates as a function of the percentage of inspired oxygen.

ratio is observed in all subjects. However, a further increase of the oxygen supply resulted in only minimal changes of the $R2*/SaO_2$ for most of the subjects.

Modeling of the R2*-response

The results of the response modeling of the GM are shown in Figure 5. The non-linear fit of the experimental data to the BOLD signal saturation curve predicts a maximum R2*response of the GM to hyperoxia equal to 3.5 % at 3 Tesla field strength (parameter A of the Hill's model). At inhalation of 68% of oxygen a response equal to the half of the maximum is expected (parameter B of the Hill's equation).

DISCUSSION

In this investigation, we showed that the quantitative response of the transverse relaxation rate of the MR signal to hyperoxic challenges in the breathing gas occurred in a concentration-dependent manner. A decrease of the GM relaxivity was already observed for slight increases in the oxygen supply (i.e. for O_2 = 50%), whereas, the relaxation rate decline levels off at oxygen concentrations in the order of 75%. Using the Hill's equation, the cerebral R2* reactivity of gray matter could be modeled providing two
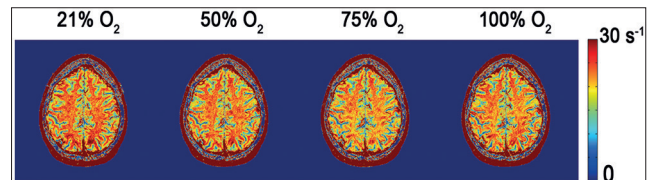
Figure 2: Exemplary R2* maps, which were computed,as for Figure 1c, from the pixel-wise fitting of multi-echo MR signals acquired using a gradient echo sequence with TR =93 ms, TE =8, 24, 40, 56, 72, 88 ms, Flip Angle =50°, voxel size =0.5 × 0.5 × 1.0 mm^3, of a central axial slice of the brain as acquired during the different stages of the respiratory challenge. A slight but significant decrease of the R2* was measured over the gray matter [Table 2]. A similar trend was observed for the white matter, which, however, was not statistically significant (P = 0.055).
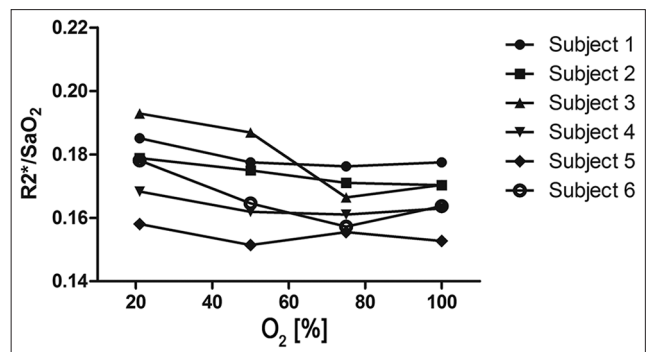
Figure 4: Visual representation of the ratios of the gray-matter R2* values divided by SaO_2 values, as a function of the percentage of inhaled oxygen. The ratio decreased when increasing the O_2 percentage from 21 to 50 % for all volunteers. However, for oxygen percentages above 75% a saturation of the R2* signal was observed.
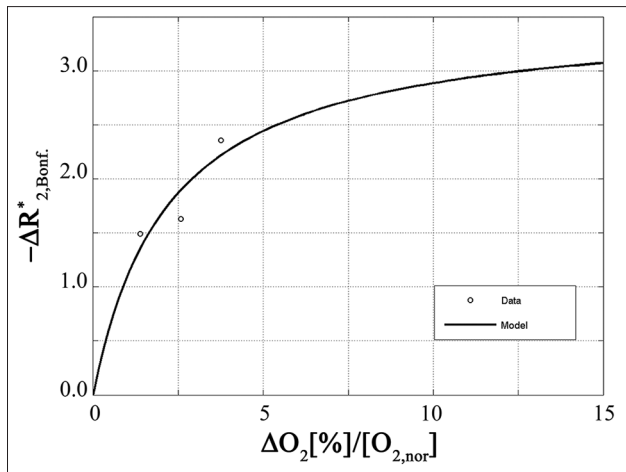
Figure 5: The mean Bonferroni-corrected gray-matter -ΔR2*-response (baseline and three gas challenges), as defined in Equation [2], as a function of the relative change in oxygen supply. A two-parameter signal saturation curve, as defined in the Equation [3]. (continuous line, 'Model') was fitted to the experimental data points (circles, 'Data'). A potential maximum asymptotic ΔR2*-response in the order of 3.5% was predicted for 3.0 Tesla, while for FiO_2 of.68 half of the maximal response could be inferred.

parameters: The maximum response A and the necessary oxygen challenge to reach 50% of the maximum response.

The results of this study indicate that even in healthy volunteers, without any history of cardiovascular or respiratory disease and with arterial blood saturation in the order of 98%, at FiO_2 of 0.21, can undergo a significant increase of cerebral tissue oxygenation, indirectly measured by the R2* of the MR-signal, by increasing the oxygen supply. Although under normal physiological conditions circa 98% of the human hemoglobin is saturated, the delivery of the oxygen to the tissue can be affected by manipulation of the partial pressure of the oxygen in the lungs.[10,26] Normalizing our R2* measurements to the individually measured SaO_2 values mirrors the physiological properties of oxygen transport. Increasing the FiO_2 to 0.50 results in an oxygen saturation of the arterial hemoglobin, which accounts for the majority of oxygen delivered to the tissue, and hence, the $R2*/SaO_2$ ratio declines in all the study subjects. Little oxygen is soluble in the plasma itself increasing the inhaled oxygen content even further.[10] However, it is tempting to speculate that the additional plasma dissolved oxygen replenishes the pool of oxyhemoglobin in the GM to some extent, which might contribute to the maximum decrease of the R2* around a FiO_2 of 0.75 compared to the normoxic conditions.

In this study, we focused on the administration of oxygen without the addition of any vasoactive agents (such as carbon dioxide or acetazolamide) in an attempt to exclusively manipulate the deoxyhemoglobin concentration.[11] On account of the vasoconstrictive properties of oxygen a slight reduction in the blood flow (partly counteracting the oxygen delivery to the tissue) has to be considered, which could also explain the subtle differences in R2* observed at a FiO_2 of 1.00 as compared to FiO_2 of 0.75. Also, Ashkanian and colleagues reported a mean change of blood flow in the gray matter in the order of 10% during breathing of 100% oxygen.[27]

Although changes in the concentration of deoxyhemoglobin seem to be the main source of the BOLD response to respiratory challenges, paramagnetic effects of the molecular oxygen dissolved in the capillary bed or in the cerebrospinal fluid, as well as the paramagnetic effects of gaseous oxygen enclosed in the upper and lower airways cannot be excluded.[28-30] Shim adjustments performed before the acquisition of each dataset for R2* quantification, the orientation of the imaged volume avoiding the upper airways, and the reduced sensibility of the signal to macroscopic field inhomogeneities, on account of the high spatial resolution of the datasets that should have mitigated the effects of molecular oxygen on the R2* measurements in this study.

This study proved the feasibility to monitor the R2*-response to graded hyperoxia at a clinically applicable field strength of 3.0 Tesla. A mean relative change in the R2* of the gray matter during breathing of 100% oxygen, in respect to normoxia of 4 to 5%, was found. This result was in good accordance with the values of the BOLD effect previously reported in the literature.[2] However, a change in the order of 4% is at the detectability limit of an MRI.[31] Some strategies may help improve the sensitivity of the R2*-response to hyperoxia. Moving to an even higher field strength provides the advantages of both, stronger BOLD contrast and higher signal-to-noise of the T2*-weighted images. On the other hand ultra-high field MRI may bring into question the clinical feasibility of the technique. A further opportunity for improving the sensitivity of the response would be to perform a block-designed respiratory challenge, which would allow a pixel-wise parametrical statistical analysis of the data.[31] In the current study, we did not apply a block design with return-to-baseline oxygen levels. The reason for this choice was to keep the measurement time with the gas mask as short as possible, to minimize the discomfort of the subjects. Boss and colleagues showed that in the kidneys the tissue oxygen concentration nearly reached equilibrium after three minutes of the gas challenge.[20] For this reason, we applied a delay of three minutes after the initiation of the gas challenge, before starting the MR acquisition. In principle, a dynamic measurement of the equilibration phase would have been advantageous. As the acquisition time of the applied GRE sequence is in the order of three minutes, and therefore not suitable for dynamic measurements, we performed pilot studies using a T2*-weighted Echo-Planar Imaging (EPI) sequence,

which, however, showed insufficient sensitivity to detect gas challenge–induced changes.

Limitations

Our study had a few limitations. (a) A relatively small number of volunteers were included in the study. The reason for this was the limited availability of the anesthesia device for research purposes. However, in spite of the small sample size, the most important parameters showed statistical significance. (b) The R2* response was not modeled in dependence of the physiological parameters, ppO_2 and $ppCO_2$, but instead with the concentration of oxygen in the breathing gas. (c) We were not able to provide estimates of the error of the parameters A and B obtained by the modeling of the R2* response, as the intra-individual variability of the responses was too high to obtain meaningful values for intra-individual fitting. Therefore, we decided to perform a fit of the mean values of the R2* responses. The reason for the strong variability is that the R2* response is at the limit of detectability with an MRI, which may change with further improvement of the MR image acquisition techniques and higher field strengths. (d) We did not dynamically acquire image data for computation of R2* responses during a wash-in, neither did we dynamically measure the physiological responses during the wash-in. In the pilot experiments, we were not able to reliably measure the dynamic R2* response using a standard T2*-weighted echo-planar imaging sequence. We do not exclude that with more advanced imaging techniques, dynamic measurements of the R2* response during wash-in may be feasible.

CONCLUSION

In conclusion, we present a technique that allows the quantification of the BOLD response of GM to increasing concentrations of oxygen in the inhaled gas. We were able to show that a hyperoxic gas challenge using pure oxygen results in a significant increase in cerebral tissue oxygenation. The possibility of monitoring the regionally specific response of the brain tissue to hyperoxia in a clinical setting may have an important impact on the management of several patient collectives. First, it may help in monitoring the response to normobaric hyperoxia therapy in patients with traumatic brain injury and stroke.[32] Second, it may help detect hypoxic areas in large, inhomogeneous tumors. This information could be used during the dose-planning phase before start of therapy, for example, with an increased target dose to these areas that are known to respond less well to therapy.[33]Third, the computation of a hyperoxic response coefficient (parameter B of the Hill's equation) may provide a deeper insight into the pathological changes of vasoreactivity in patients with degenerative neurological disorders, such as, Alzheimer's disease or other diseases causing dementia.

ACKNOWLEDGMENTS

REFERENCES

1. Rostrup E, Larsson HB, Toft PB, Garde K, Henriksen O. Signal changes in gradient echo images of human brain induced by hypo- and hyperoxia. NMR Biomed 1995;8:41-7.
2. Rossi C, Boss A, Donati OF, Luechinger R, Kollias SS, Valavanis A, et al. Manipulation of cortical gray matter oxygenation by hyperoxic respiratory challenge: Field dependence of R (2) * and MR signal response. NMR Biomed 2012;25:1007-14.
3. Kennan RP, Scanley BE, Gore JC. Physiologic basis for BOLD MR signal changes on account of hypoxia/hyperoxia: Separation of blood volume and magnetic susceptibility effects. Magn Reson Med 1997;37:953-6.
4. Schenck JF. The role of magnetic susceptibility in magnetic resonance imaging: MRI magnetic compatibility of the first and second kinds. Med Phys 1996;23:815-50.
5. Davis TL, Kwong KK, Weisskoff RM, Rosen BR. Calibrated functional MRI: Mapping the dynamics of oxidative metabolism. Proc Natl Acad Sci U S A 1998;95:1834-9.
6. Hoge RD, Atkinson J, Gill B, Crelier GR, Marrett S, Pike GB. Investigation of BOLD signal dependence on cerebral blood flow and oxygen consumption: Thedeoxyhemoglobin dilution model. Magn Reson Med 1999;42:849-63.
7. Chiarelli PA, Bulte DP, Wise R, Gallichan D, Jezzard P. A calibration method for quantitative BOLD fMRI based on hyperoxia. Neuroimage 2007;37:808-20.
8. Henninger N, Bouley J, Nelligan JM, Sicard KM, Fisher M.Normobaric hyperoxia delays perfusion/diffusion mismatch evolution, reduces infarct volume, and differentially affects neuronal cell death pathways after suture middle cerebral artery occlusion in rats. J Cereb Blood Flow Metab 2007;27:1632-42.
9. Santosh C, Brennan D, McCabe C, Macrae IM, Holmes WM, Graham DI, et al. Potential use of oxygen as a metabolic biosensor in combination with T2*-weighted MRI to define the ischemic penumbra. J Cereb Blood Flow Metab 2008;28:1742-53.
10. Sjöberg F, Singer M. The medical use of oxygen: A time for critical reappraisal. J Intern Med 2013;274:505-28.
11. Fierstra J, Sobczyk O, Battisti-Charbonney A, Mandell DM, Poublanc J, Crawley AP, et al. Measuring cerebrovascular reactivity: What stimulus to use? J Physiol 2013;591:5809-21.
12. Hare HV, Germuska M, Kelly ME, Bulte DP. Comparison of CO2 in air versus carbogen for the measurement of cerebrovascular reactivity with magnetic resonance imaging. J Cereb Blood Flow Metab 2013;33:1799-805.
13. Prisman E, Slessarev M, Han J, Poublanc J, Mardimae A, Crawley A, et al. Comparison of the effects of independently-controlled end-tidal PCO (2) and PO (2) on blood oxygen level-dependent (BOLD) MRI. J Magn Reson Imaging 2008;27:185-91.
14. Losert C, Peller M, Schneider P, Reiser M. Oxygen-enhanced MRI of the brain. Magn Reson Med 2002;48:271-7.
15. Ben Bashat D, Artzi M, Ben Ami H, Aizenstein O, Blumenthal DT, Bokstein F, et al. Hemodynamic response imaging: A potential tool for the assessment of angiogenesis in brain tumors. PLoS One 2012;7:e49416.
16. Robinson SP, Rodrigues LM, Howe FA, Stubbs M, Griffiths JR. Effects of

different levels of hypercapnic hyperoxia on tumour R (2)* and arterial blood gases. Magn Reson Imaging 2001;19:161-6.

17. Müller A, Remmele S, Wenningmann I, Clusmann H, Träber F, Flacke S, et al. Analysing the response in R2* relaxation rate of intracranial tumours to hyperoxic and hypercapnic respiratory challenges: Initial results. Eur Radiol 2011;21:786-98.

18. Punwani S, Ordidge RJ, Cooper CE, Amess P, Clemence M. MRI measurements of cerebral deoxyhaemoglobin concentration [dHb]–correlation with near infrared spectroscopy (NIRS). NMR Biomed 1998;11:281-9.

19. Mürtz P, Flacke S, Müller A, Soehle M, Wenningmann I, Kovacs A, et al. Changes in the MR relaxation rate R2* induced by respiratory challenges at 3.0 T: A comparison of two quantification methods. NMR Biomed 2010;23:1053-60.

20. Boss A, Martirosian P, Jehs MC, Dietz K, Alber M, Rossi C, et al. Influence of oxygen and carbogen breathing on renal oxygenation measured by T2*-weighted imaging at 3.0 T. NMR Biomed 2009;22:638-45.

21. Oliphant TE. Python for Scientific Computing. Comput Sci Eng 2007;9:10-20.

22. Zhang Y, Brady M, Smith S. Segmentation of brain MR images through a hidden Markov random field model and the expectation-maximization algorithm. IEEE Trans Med Imaging 2001;20:45-57.

23. Smith SM. Fast robust automated brain extraction. Human Brain Mapp 2002;17:143-55.

24. Goutelle S, Maurin M, Rougier F, Barbaut X, Bourguignon L, Ducher M, et al. The Hill equation: A review of its capabilities in pharmacological modelling. Fundam Clin Pharmacol 2008;22:633-48.

25. Bernstein MA, King KF, Zhou XJ. Handbook of MRI Pulse Sequences. Burlington: Academic Press Inc.; 2004. p. 433-7.

26. Thomas D. The physiology of oxygen delivery. Vox Sang 2004;87(Suppl 1):70-3.

27. Ashkanian M, Borghammer P, Gjedde A, Ostergaard L, Vafaee M. Improvement of brain tissue oxygenation by inhalation of carbogen. Neuroscience 2008;156:932-8.

28. Raj D, Paley DP, Anderson AW, Kennan RP, Gore JC. A model for susceptibility artefacts from respiration in functional echo-planar magnetic resonance imaging. Phys Med Biol 2000;45:3809-20.

29. Pilkinton DT, Gaddam SR, Reddy R. Characterization of paramagnetic effects of molecular oxygen on blood oxygenation level-dependent-modulated hyperoxic contrast studies of the human brain. Magn Reson Med 2011;66:794-801.

30. Song Y, Cho G, Chun SI, Baek JH, Cho H, Kim YR, et al. Oxygen-induced frequency shifts in hyperoxia: A significant component of BOLD signal. NMR Biomed 2014;27:835-42.

31. Uludag K, Dubowitz DJ, Buxton RB. Basic principles of functional MRI. In: Edelman R, Hesselink J, Zlatkin M, editors. Clinical MRI. San Diego: Elsevier; 2005. p. 249-87.

32. Yuan Z, Liu W, Liu B, Schnell A, Liu KJ. Normobaric hyperoxia delays and attenuates early nitric oxide production in focal cerebral ischemic rats. Brain Res 2010;1352:248-54.

33. Jamin Y, Glass L, Hallsworth A, George R, Koh DM, Pearson AD, et al. Intrinsic susceptibility mri identifies tumors with ALKF1174L mutation in genetically-engineered murine models of high-risk neuroblastoma. PLoS One 2014;25:e92886.